

Fish scale terrace GaInN/GaN light-emitting diodes with enhanced light extraction

Christoph J. M. Stark,¹ Theeradetch Detchprohm,¹ Liang Zhao,¹ Tanya Paskova,^{2,a)} Edward A. Preble,² and Christian Wetzel¹

¹*Future Chips Constellation and Department of Physics, Applied Physics, and Astronomy, Rensselaer Polytechnic Institute, Troy, New York 12180, USA*

²*Kyma Technologies, Inc., 8829 Midway West Road, Raleigh, North Carolina 27617, USA*

(Received 5 September 2012; accepted 15 November 2012; published online 5 December 2012)

Non-planar GaInN/GaN light-emitting diodes were epitaxially grown to exhibit steps for enhanced light emission. By means of a large off-cut of the epitaxial growth plane from the *c*-plane (0.06° to 2.24°), surface morphologies of steps and inclined terraces that resemble fish scale patterns could controllably be achieved. These patterns penetrate the active region without deteriorating the electrical device performance. We find conditions leading to a large increase in light-output power over the virtually on-axis device and over planar sapphire references. The process is found suitable to enhance light extraction even without post-growth processing. © 2012 American Institute of Physics. [<http://dx.doi.org/10.1063/1.4769442>]

GaN-based light emitting diodes (LEDs) are poised to displace conventional incandescent and fluorescent lighting on the grounds of higher energy efficiency and reliability. In a first generation, a combination of blue LEDs and rare earth phosphors was used to create light that appears white to the human eye when directly looked at. Next, however, better color rendering, higher efficiency, and lower cost will be achieved by phosphor-free composite white lamps that separately provide several colors by direct emitting LEDs.¹ For the high optical power densities required, preference must be given to epitaxial approaches that already include the light extraction design. Optical waveguiding in standard planar structures is prone to the trapping of light and thereby reducing overall efficiency.² Approaches to overcome those limitations include patterning of a transparent substrate, e.g., LEDs on patterned sapphire³ or to roughen the emission surface of the epilayer itself, e.g., by crystallographic wet etching of the N-face GaN surface of flip-chip LEDs.⁴ In other methods, the p-doped GaN layer or the p-contact is roughened.^{5,6}

It can be speculated that light extraction should be most efficient when the pattern penetrates the active region itself.⁷ Any top-down etching process, however, is likely to introduce defects in the active region that leads to non-radiative losses and increased leakage current. Therefore, we here present a method by which a patterning of the active region is introduced bottom-up during the epitaxial growth. We show that this can be achieved on highly off-cut GaN templates.

c-plane grown bulk GaN templates (size 1 cm^2) were prepared to various off-cut (or miscut) angles. Per inspection, this miscut occurred in a direction approximately along $\langle 21\bar{1}0 \rangle$. Off-cut angles of 0.06° , 0.70° , and 2.24° were obtained as specified by the maximum value across the sample piece. The substrates then were chemo-mechanically polished (CMP) on both *c*-sides. For comparison, a reference planar GaN template on single-side polished sapphire was prepared. That sapphire had a 0.25° off-cut towards the

m-direction, specified as a wafer mean value. Before initiating homoepitaxy, the bulk GaN pieces were slightly etched in hot AZ400K for 10 min and then cleaned in hydrofluoric acid for 10 min. This step also creates features of pyramidal shapes on the N-face backside to a roughness of $1\text{ }\mu\text{m}$ (root mean square (RMS)), similar to the backside of the sapphire wafer. On the front side, however, no changes to the smooth surface are observed. Then, full LED structures were grown by metal organic vapor phase epitaxy (MOVPE). The structure includes an n-GaN layer, 8 pairs of GaInN/GaN quantum wells (QWs), a Mg-doped-AlGaIn electron-blocking layer, and a p-GaN top layer.⁸ After Mg-dopant activation, LED dies of size $350 \times 350\text{ }\mu\text{m}^2$ were fabricated. A mesa was formed by inductively coupled plasma reactive ion etch (ICP-RIE) in Cl_2/BCl_3 chemistry. Ti/Al/Ti/Au (20 nm/100 nm/45 nm/55 nm) was deposited as n-contact and annealed in N_2 , and semitransparent Ni/Au (5 nm/5 nm) was used as p-contact and annealed in O_2 . For best possible direct comparison, the LEDs on 0.06° and 0.70° off-cut GaN as well as on the sapphire-based template were grown in the same epitaxy run. The structure on 2.24° off-cut GaN was grown in a separate, but nominally identical run. Resulting structures are laboratory-scale epitaxy samples of typical LED geometry. These samples and resulting performance characteristics should not be confused with fully fabricated, encapsulated, packaged, and properly cooled LED lamps as available commercially.

An upper limit of the internal quantum efficiency (IQE) as a function of laser irradiance was determined by dividing the photoluminescence (PL) efficiency at room temperature by the maximum PL efficiency at 4 K. Here, the PL efficiency is given by the ratio of PL intensity to the external excitation laser intensity. For excitation, a 405 nm laser was chosen to excite the QWs directly, but not the GaN barrier and contact layers. Cathodoluminescence (CL) was performed at room temperature with an acceleration voltage of 10 kV. Electroluminescence (EL) was collected from the substrate side into the 1 cm diameter entrance of an integrating sphere and analyzed by a CCD-spectrometer. The measurement system was spectrally calibrated using a NIST-traceable light source.

^{a)}Present address: Materials Science and Engineering Department, North Carolina State University, Raleigh, North Carolina 227695, USA.

All completed structures show a pronounced step-like surface pattern in optical microscopy in Nomarski mode (Figs. 1(a)–1(d)). In particular, the material with the highest off-cut angle of 2.24° shows a pronounced pattern resembling fish scales (Fig. 1(c)) with steps found oriented roughly perpendicular to the approximately $\langle 2\bar{1}\bar{3}0 \rangle$ off-cut direction. The surface morphology of the 0.06° off-cut (Fig. 1(a)) and the 0.70° off-cut (Fig. 1(b)) templates, however, shows step-like features that run along an $[2\bar{1}\bar{1}0]$ a -axis of GaN, i.e., it seems decoupled from the off-cut direction. Surface height profiles were taken with a stylus profilometer along a path across the steps (Figs. 1(e)–1(h)). The profiles reveal quasi-periodic asymmetric trapezoidal surface features. The linear height variations can be described by a surface roughness yielding values of 16 nm RMS (0.06° off-cut), 28 nm RMS (0.70°), 66 nm RMS (2.24°), and 9 nm RMS (0.25°). The difference in surface roughness is also evident in the microscope images in Figs. 1(a) and 1(b). From the profile traces, the slopes of the terraces are estimated as 0.27° (0.06° off-cut), 0.16° (0.70°), and 1.6° (2.24°). Apparently, the off-cut angle is well preserved throughout the full LED structure growth only for the 2.24° off-cut substrate.

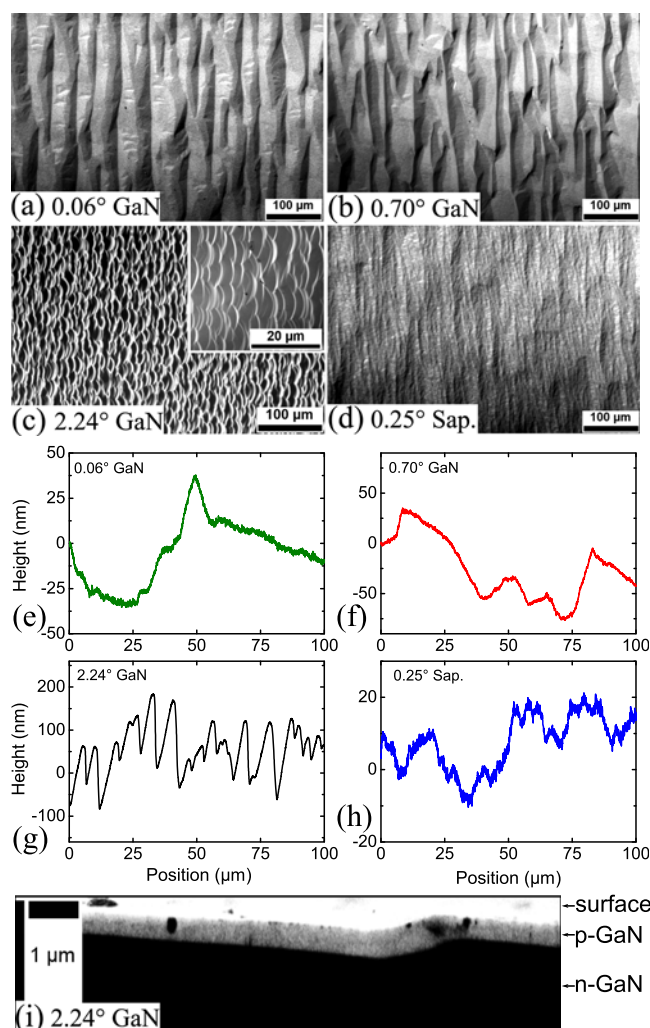


FIG. 1. Surface morphology after LED growth on off-cut GaN and sapphire. (a)–(d) Nomarski microscope images revealing step-like patterns. The inset shows a magnified view of (c). (e) and (f) Surface profiles showing steps and terrace structures. (i) SEM cross-section of 2.24° off-cut LED.

The observed patterns are not just a surface feature. A cross-sectional SEM image (Fig. 1(i), 2.24° off-cut) reveals that the interface of active region and p-GaN, to a large extent, runs parallel to the patterned top surface. Apparently, the QWs themselves must have grown in a non-planar configuration. The steps at the terrace edges have a finite slope and therefore include crystallographic planes different from the terrace tops. Both aspects may lead to a distinctive behavior of the LED performance.

The spatial wavelength distribution was studied by CL (Fig. 2). The area-integrated spectra (Fig. 2(g)) on a log intensity scale show a wide wavelength distribution in all structures. Peak wavelengths of 503 nm (0.06° off-cut), 507 nm (0.70°), 485 nm (2.24°), and 514 nm (0.25°) are found. The maximum signal in the bulk GaN-based material is slightly lower than in the sapphire-based reference. The CL spatial maps of the 2.24° off-cut material (Figs. 2(a)–2(c)) show strong emission near the step edges. Apparently, emission from areas of steep slopes dominates over that of flat areas. This feature is pronounced when analyzing the CL intensity map at 485 nm, the wavelength of the peak emission (Fig. 2(b)). At shorter wavelength, the same distribution is seen (Fig. 2(a), 470 nm), while contrast is weaker for longer wavelength (Fig. 2(c), 500 nm). For the 0.70° off-cut material, the monochromatic CL intensity map at 507 nm

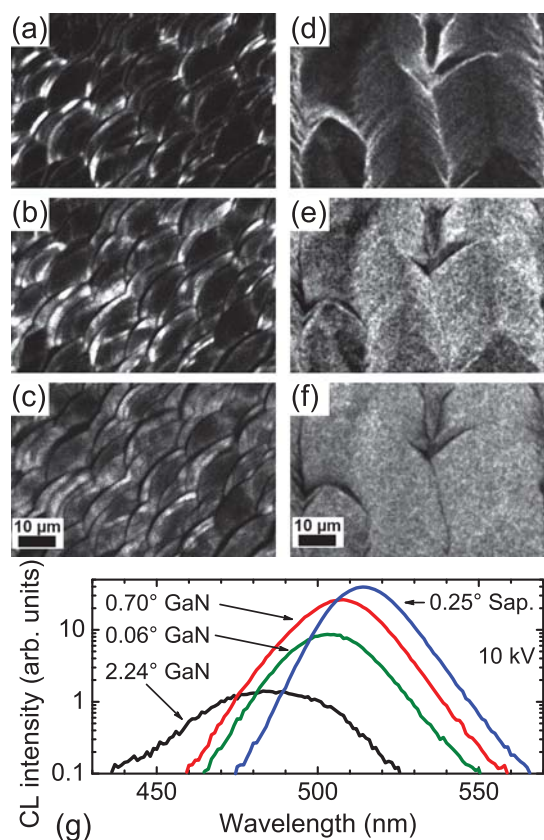


FIG. 2. Monochromatic CL intensity maps for (a)–(c) 2.24° off-cut and (d)–(f) 0.70° off-cut samples after full LED growth. The detection wavelengths are (a) 470 nm, (b) 485 nm (emission peak), (c) 500 nm, (d) 490 nm, (e) 507 nm (emission peak), and (f) 520 nm. For both structures, it is evident that the correlation of the emission with the surface features is the strongest for the shorter wavelength tail. If (d) and (f) are compared, the emission patterns are found to be complementary. (g) Integrated CL spectra of all four samples.

(Fig. 2(e)) shows a spatial correlation with the surface morphology features of that structure (Fig. 1). The shorter wavelength emission side (Fig. 2(d)) exhibits intensity maxima in repeating patterns along the edges of the inclined step features, while the longer wavelength emission side is uniformly distributed in the remaining areas (Fig. 2(f)). These features on the 0.70° LED are markedly different from those on the 2.24° off-cut LED, however, common to both structures is a peak emission intensity that strongly correlates spatially with the top surface morphology. This proves that the active QW regions themselves already contain the patterns, which are then replicated in the observed surface patterns.

The morphology patterns should also affect LED device performance. Light output power (LOP) vs. current density for the different structures is shown in Fig. 3. At a current density of 50 A/cm², the following LOP was obtained: 1.1 mW (0.06° off-cut), 3.4 mW (0.70°), 4.1 mW (2.24°) on GaN, and 1.8 mW (0.25°) on sapphire. The forward voltage at this current density was 6.9 V (0.06° off-cut), 6.2 V (0.70°), 13 V (2.24°), and 5.3 V (0.25°). The reverse leakage current at -5 V was less than 8 μA for all devices. Apparently, within the GaN-based LED set the output power increases with increasing off-cut angle by up to 3.7 times. This trend clearly dominates over any observed die-to-die variations. The maximum, achieved at 2.24° off-cut, exceeds the sapphire based reference structure by a factor of 2.2 at 50 A/cm². The far-field pattern of the top surface EL was analyzed in all samples. The intensity maximum was observed at various angles in reference to the macroscopic wafer normal: 3.5° (0.06° off-cut), 1.8° (0.70°), and 9.5° (2.24°). While the distinction between the first two values may lie in the limits of the alignment accuracy of the die, the later value clearly sticks out. Apparently, this deviation is of the order of the inclination of the *c*-plane growth surfaces. The external quantum efficiency (EQE) for the 2.24° off-cut structure (Fig. 4(a)) reaches 4.7% (at 10 A/cm²) despite collecting only light emitted through the bare substrate backside in this experiment. Under variation of current density from 5 to 50 A/cm², a wavelength blue-shift of 10–15 nm is seen in all samples. The peak wavelengths at 50 A/cm² are 499 nm (0.06° off-cut), 505 nm (0.70°), 471 nm (2.24°), and 509 nm

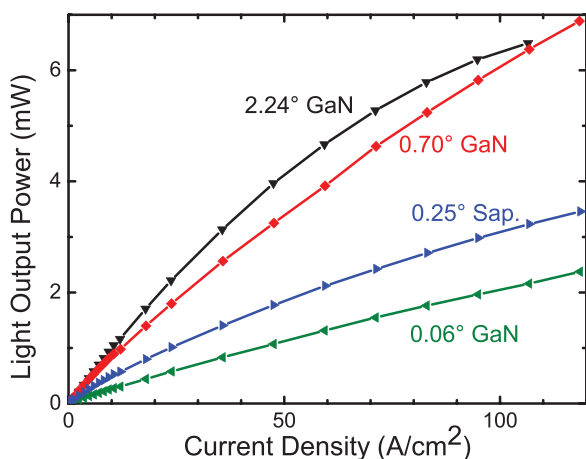


FIG. 3. Light output power as function of drive current density for the different structures. The LED on 2.24° off-cut GaN shows the best performance over a wide range of current densities.

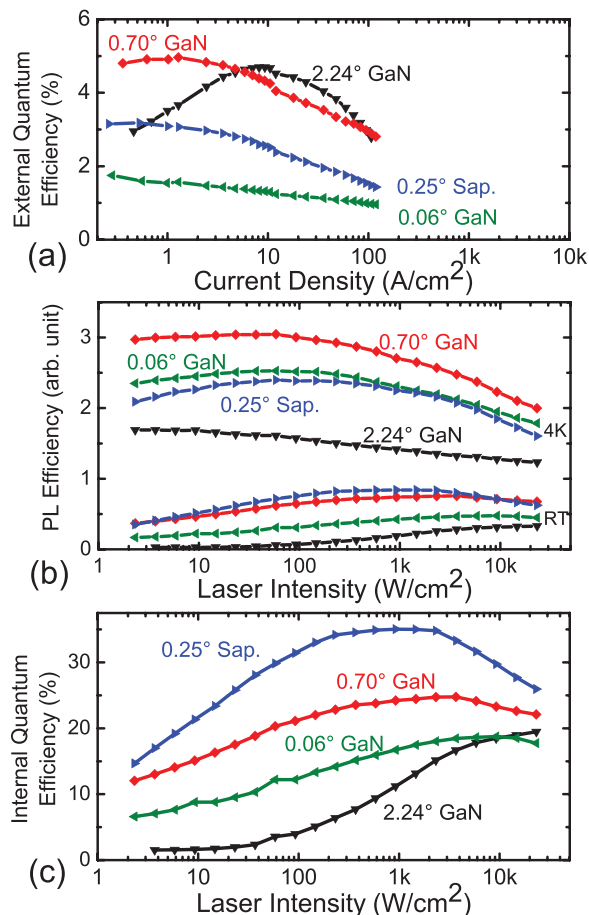


FIG. 4. (a) EQE as function of drive current density. (b) PL efficiencies at 4K and room temperature (RT) as function of laser irradiance. (c) Upper limit of IQE calculated from the data in (b). The IQE curves mostly reflect the PL efficiency trends at RT. The LEDs on 0.70° and 2.24° off-cut GaN show higher EQE than the reference on sapphire for high current density, but overall have lower IQE.

(0.25°). The high forward voltage (V_f), especially for the 2.24° off-cut LED, is believed to be a result of non-optimal doping conditions in the contact layers. A high V_f leads to Joule heating, and an increased temperature may have some effect on efficiency.⁹ If the patterns were to introduce additional defects in the active layer, the corresponding increased leakage current should have lowered the forward voltage. Since this is not the case, we conclude the achievement of terrace patterning without the introduction of leakage paths.

PL as a function of excitation laser pump intensity of the LEDs on GaN is compared to the sapphire reference in Fig. 4(b) and interpreted in terms of an upper limit of IQE in Fig. 4(c). For the given arrangements, we estimate that a pump intensity of 100 W/cm² corresponds to a current density of about 5 A/cm². The 2.24° off-cut device shows a saturation of both, PL efficiency and derived IQE within the measured excitation range, and overall has the lowest PL efficiency and IQE. The LED on 0.70° off-cut GaN shows the best IQE of the devices on GaN, but the 0.25° off-cut sapphire reference reaches the highest absolute values. In terms of PL efficiencies, however, both are comparable at room temperature. At highest excitation densities, the 0.70° GaN-based device is slightly better. The 2.24° off-cut device shows both, the lowest PL efficiency and lowest IQE.

An interpretation of these results should not aim at a performance comparison between GaN- and sapphire-based LEDs since both substrates induce different defect densities and light extraction efficiencies, which cannot be controlled for here. Instead, the comparison shall provide evidence of the relevance of the differentiation within the GaN-based structures by means of the fish scale terrace approach. The results of primary interest are those of EL. They do not reflect the trends seen in PL well. This suggests that either current injection or optical excitation conditions may vary from sample to sample. Such a finding is not unexpected and emphasizes the need for multiple characterization approaches. We find that the LED with the highest off-cut angle of 2.24° , which also has the largest surface roughness, shows the highest EQE over a range of medium current densities. This in part must be attributed to the shorter emission wavelength obtained, about 30 nm shorter than the 0.70° off-cut LED. The 0.70° off-cut structure, however, maintains a 3.0-fold power advantage (at 50 A/cm^2) over the virtually on-axis substrate (0.06°). The LED on sapphire can serve as reference for the device performance at similar wavelength. The performance of this reference lies in meaningful agreement with the overall trend of our standard LED epi performance. Yet, its performance should not be confused with that of fully fabricated commercial LED lamps, where aspects such as die size, encapsulation, packaging, and cooling have been optimized. Within the meaningful comparison, the superior performance of the two highly off-cut LEDs shows that strong texturing of the active region and top surface has benefits over smoother layers. In PL, the 2.24° off-cut structure shows the lowest efficiency, indicating strong non-radiative recombination even at low temperature. This is in line with the low values seen in the derived upper limit of IQE and could be related to the inhomogeneous distribution of CL emission along the terrace steps (see Figs. 2(a) and 2(b)), where the dark areas on the terrace edges are attributed to non-radiative recombination.

While the fish scale patterns seem to be controlled to run perpendicular to the off-cut direction, the patterns on the lower off-cut structures (0.06° and 0.70°) do not appear to be controlled in this way. Therefore, we propose that the driving force behind the formation of the fish scale pattern is the large angle of off-cut. By using substrates with different off-cut angles, the surface morphology could be controlled and it is believed that the increased light output results from increased light scattering at the patterns and the wedge shaping of the sample on a macroscopic length scale. The current patterns are on the order of micrometers, and additional roughening on the nanometer scale could be employed. We speculate that such a double patterning can enhance light extraction even more.

The use of off-cut substrate in heteroepitaxy of GaN-based LEDs on sapphire has been reported in the literature. However, in that case, a decreasing device performance has been found when the off-cut was increased¹⁰ from 0.2° to 1.0° , and attributed to the generation of high densities of misfit and threading dislocations. In the here presented case, however, epitaxy occurs on the smooth *c*-plane oriented terraces of GaN, while the overall sample miscut is established only as individual steps on a macroscopic length scale. The mode of epitaxial growth, therefore, should primarily be identical to the well established *c*-plane cases. Apparently, the approach so far seems to work better on bulk GaN based material in homo-epitaxy.

In summary, we have demonstrated that growth of LEDs on substrates with rather large off-cut angles leads to self-organizing patterns, the details of which depend on the magnitude and direction of off-cut inclination. Within the GaN substrate set, the LOP of such LEDs was highest for the 2.24° off-cut LED. It showed a 3.7-fold improvement compared to the LED on the smallest off-cut substrate, and a 2.2-fold increase compared to the sapphire-based reference. The patterns are found to penetrate the active region without introducing relevant current electrical leakage. From comparing IQE and EQE, we assign the performance enhancement to be primarily the result of enhanced light extraction in the induced trapezoidal growth and corresponding surface morphology. The approach should be useful for a wide range of future device designs in the area of energy efficient solid state lighting.

This work was supported by a DOE/NETL Solid-State Lighting Contract of Directed Research under DE-EE0000627. This work was supported in part by the Engineering Research Centers Program of the National Science Foundation under NSF Cooperative Agreement No. EEC-0812056 and in part by New York State under NYSTAR Contract No. C090145.

¹C. Wetzel and T. Detchprohm, *Opt. Express* **19**(S4), A962 (2011).

²J. J. Wierer, A. David, and M. M. Megens, *Nat. Photonics* **3**, 163 (2009).

³E.-H. Park, J. Jang, S. Gupta, I. Ferguson, C.-H. Kim, S.-K. Jeon, and J.-S. Park, *Appl. Phys. Lett.* **93**, 191103 (2008).

⁴T. Fujii, Y. Gao, R. Sharma, E. L. Hu, S. P. DenBaars, and S. Nakamura, *Appl. Phys. Lett.* **84**, 855 (2004).

⁵C. Tsai, J. Sheu, W. Lai, Y. Hsu, P. Wang, C. Kuo, C. Kuo, S. Chang, and Y. Su, *IEEE Electron Device Lett.* **26**, 464 (2005).

⁶P. Wang, Z. Gan, and S. Liu, *Opt. Laser Technol.* **41**, 823 (2009).

⁷S. X. Jin, J. Li, J. Y. Lin, and H. X. Jiang, *Appl. Phys. Lett.* **77**, 3236 (2000).

⁸T. Detchprohm, M. Zhu, Y. Xia, Y. Li, W. Zhao, J. Senawiratne, and C. Wetzel, *Phys. Status Solidi C* **5**, 2207 (2008).

⁹A. Laubsch, M. Sabathil, W. Bergbauer, M. Strassburg, H. Lugauer, M. Peter, S. Lutgen, N. Linder, K. Streubel, J. Hader, J. V. Moloney, B. Pasenow, and S. W. Koch, *Phys. Status Solidi C* **6**, S913 (2009).

¹⁰Y.-J. Liu, T.-Y. Tsai, C.-H. Yen, L.-Y. Chen, T.-H. Tsai, C.-C. Huang, T.-Y. Chen, C.-H. Hsu, and W.-C. Liu, *Opt. Express* **18**, 2729 (2010).